Macromolecular Nanotechnology

# Silver fillers aspect ratio influence on electrical and thermal conductivity in PEEK/Ag nanocomposites

Lisa Rivière [a], Antoine Lonjon [a], Eric Dantras [a,*], Colette Lacabanne [a], Philippe Olivier [b], Nathalie Rocher Gleizes [b]

[a] *Physique des Polymères, CIRIMAT, Université de Toulouse, CNRS, INPT, Université Toulouse 3 Paul Sabatier, Bât 3R1B2, 118, Route de Narbonne, 31062 Toulouse Cedex 9, France*
[b] *Institut Clément Ader, 3, Rue Caroline Aigle, 31400 Toulouse, France*

*Keywords:*
Thermal conductivity
Electrical conductivity
Silver nanowire
Aspect ratio
Composite

A B S T R A C T

The development of polymer based conductive composites is required in aeronautical applications where electrostatic charges and heat need to be evacuated. Optimization of conductive filler content is necessary to maintain low density and high mechanical properties provided by the polymer matrix. We introduced silver nanoparticles in Polyetheretherketone. Electrical conductivity, specific heat capacity, thermal conductivity and thermal diffusivity have been determined as a function of filler content and temperature. In particular, we studied the influence of silver nanoparticles aspect ratio on these thermal properties. We compared nanospheres with nanowires. A low electrical percolation threshold (0.55 vol%) is obtained for silver nanowires composites compared to spherical particles (10.8 vol%). Thermal conductivity increases with silver content and the influence of filler aspect ratio is interesting: thanks to nanowires, the thermal conductivity enhancement is reached for lower silver content. Experimental data are well fitted with Nan model. Specific heat capacity decreases with the introduction of silver nanoparticles, following the mixture rule independently of aspect ratio. Composites thermal diffusivity also increases with increasing silver content and influence of filler aspect ratio can be brought to light. Temperature dependence of these thermal properties indicate a dominant heat transport mechanism typical of disordered materials.

## 1. Introduction

Thermostable thermoplastic based composites are attractive in aeronautical applications for their low density, recyclability and high mechanical properties. However, polymer matrices are insulators, they hinder heat and electrostatic charges flow. The development of thermally and electrically conductive matrices, while maintaining low density and mechanical properties is therefore needed. The interesting use of high aspect ratio conductive filler has been demonstrated in the improvement of electrical conductivity, and electric charges transport mechanisms in insulator/conductor composites are well understood [1–3]. Highly conductive, low filled polymer based composites can be obtained with carbon nanotubes [4] and metallic nanowires [5–7].

* Corresponding author.
*E-mail address:* eric.dantras@univ-tlse3.fr (E. Dantras).

http://dx.doi.org/10.1016/j.eurpolymj.2016.08.003 .

The introduction of thermally conductive filler in polymer matrices appears to increase thermal conductivity [8–11]. Many studies have been devoted to carbon fillers with various shapes. Carbon nanotubes composites exhibit higher thermal conductivity than carbon black or short fibers composites [12–14]. This behaviour has been attributed to nanotubes high intrinsic thermal conductivity and aspect ratio [15,16]. Nan et al. [17] predicted the influence of filler aspect ratio on thermal conductivity with a model based on the classical Maxwell-Garnet effective medium approximation [18] in which interfacial thermal resistances are considered.

Fewer studies concern high aspect ratio metallic particles for thermal conductivity enhancement. Zeng et al. [19,20] used copper and silver nanowires in organic phase change materials to increase thermal conductivity. Chen et al. [21] and Razeeb and Dalton [22] investigated thermal properties of aligned cobalt and copper nanowires arrays embedded in polymer matrix for thermal interface materials. To the best of our knowledge, randomly dispersed silver nanowires have never been investigated to improve thermal conductivity of thermostable thermoplastics.

In this paper, we propose to study the influence of silver nanoparticle aspect ratio on electrical and thermal transport properties of polyetheretherketone/silver (PEEK/Ag) nanocomposites. In particular, we compared silver spherical nanoparticles and high aspect ratio nanowires. Composites electrical charges transport was compared, and electrical percolation parameters analysed regarding conductive particles morphology and dispersion. Thermal transport in PEEK/Ag nanocomposites has been evaluated through the determination of specific heat capacity $C_p$, thermal conductivity $\lambda$ and thermal diffusivity $\alpha$ as a function of particle content and temperature. Composite specific heat capacity was determined by modulated temperature differential scanning calorimetry, thermal conductivity by the guarded hot plates method and thermal diffusivity by laser flash analysis. Temperature dependence of thermal properties was investigated in order to identify the dominant heat transport mechanisms below polymer matrix glass transition temperature.

## 2. Experimental

### 2.1. Composites processing

A homogenous blend of PEEK powder (Vestakeep 2000PF, Evonik) and silver nanoparticles dispersed in ethanol, was dried in a rotary vacuum evaporator. The dry mixture was hot pressed at 380 °C for 15 min, to produce bulk PEEK/Ag nanocomposites disks. In the case of PEEK/AgNP composites, disks were cut into pellets and pressed again until homogenization. In the case of PEEK/AgNWs composites, samples are directly processed from hot pressed powder. Spherical silver nanoparticles (AgNP) from Sigma Aldrich have a mean diameter inferior to 100 nm and an aspect ratio of about 1. Silver nanowires (AgNWs) were elaborated by polyol process [6] in our laboratory. They have a mean length of 40 μm, a mean diameter of 180 nm and an aspect ratio $\xi = L/d$ of about 220. Nanowires dimensions were estimated by statistical counting from scanning electron microscopy (SEM) images [7].

### 2.2. Analysis techniques

#### 2.2.1. Volumic mass and Ag content determination

Samples volumic mass was determined by a suspension method based on Archimedes' principle [23]. The sample is suspended with a polyamide thread into a container of water placed on an electronic scale. Sample volume equals the volume of displaced water. This volume corresponds to the mass increase $\Delta m = m_2 - m_1$ recorded by the scale when the sample is immersed. Knowing the sample mass $m_{sample}$ and water volumic mass $\rho_{water}$, sample volumic mass $\rho_{sample}$ was calculated with Eq. (1).

$$\rho_{sample} = \frac{m_{sample}}{\Delta m} \times \rho_{water} = \frac{m_{sample}}{m_2 - m_1} \times \rho_{water} \quad (1)$$

$m_1$ is the recorded mass before sample immersion and $m_2$ the mass after sample immersion. The accuracy of this method relies on the fact that the forces applied on the sample are balanced.

Ag volume content $x$ was deduced from Eq. (2) with $\rho_{PEEK} = 1.28$ g cm$^{-3}$ and $\rho_{Ag} = 10.3$ g cm$^{-3}$

$$\rho_{sample} = x\rho_{Ag} + (1 - x)\rho_{PEEK} \quad (2)$$

PEEK/AgNWs composites (10 samples) with particles content from 0.5 vol% (4.1 wt%) to 7.8 vol% (40.4 wt%) and PEEK/AgNP (7 samples) with particles content from 1.3 vol% (9.5 wt%) to 15.6 vol% (59.5 wt%) were elaborated.

#### 2.2.2. Morphological analysis

Scanning eletron microscopy (SEM) observation has been carried out in order to analyse silver particles dispersion in nanocomposites. The microscope JSM 6700F (JEOL, Japan), equipped with field emission gun, at a voltage of 10 kV has been used. Observations have been made on cryo-fractured samples, perpendicularly to their surface. Backscattered electron detector has been selected to show density contrast between silver and PEEK.

*2.2.3. DC electrical conductivity*

DC electrical conductivity of insulating composites (Z > 10 Ω) was determined by dielectric spectroscopy with a Novocontrol broadband dielectric spectrometer (with SI 1260 gain/phase analyser). Experiments were carried out on sample disks with a diameter of 20 mm and a thickness of 500 μm, at 20 °C in the frequency range $10^{-2}$–$10^{6}$ Hz. Samples were coated with silver ink and placed between 10 mm gold plated electrodes.

In disordered solids, real part of the measured electrical conductivity $\sigma'(\omega)$ is frequency dependant following Eq. (3):

$$\sigma'(\omega) = \sigma_{DC} + A\omega^{s} \tag{3}$$

As the term $A\omega^{s}$ becomes negligible when $\omega$ tends to zero, we made the approximation that at $10^{-2}$ Hz, the real part of the measured electrical conductivity $\sigma'(10^{-2}\ \text{Hz})$ is equivalent to DC conductivity $\sigma_{DC}$.

For conductive composites (Z < 10 Ω), resistivity was measured with a Keithley 2420 ohmmeter in the four wires configuration. Samples were disks with a diameter of 50 mm and thicknesses varying from 2.09 to 2.43 mm coated with silver ink and placed between two 20 mm gold plated electrodes. Resistivity of compressed silver nanowires was also measured with this technique.

Thermal conductivity λ, thermal diffusivity α and specific heat capacity $C_p$, are linked by Eq. (4), deduced from the linearized Fourier's heat equation.

$$\alpha = \frac{\lambda}{\rho C_p} \tag{4}$$

In this work, these three parameters have been measured independently.

*2.2.4. Thermal conductivity*

A guarded hot plates apparatus (DTC300, TA Instruments) has been used to measure composite thermal conductivity. Samples were disks with a diameter of 50 mm and thicknesses varying from 2.09 to 2.43 mm coated with silicone based conductive compound. Measurements were performed at 25 °C, 50 °C and 80 °C, below the PEEK glass transition temperature ($T_g$ = 145 °C) [24].

According to Fourier's law, thermal conductivity λ is determined with Eq. (5):

$$\lambda = -\frac{\phi}{\Delta T} \times \frac{e}{S} \tag{5}$$

The sample with a thickness $e$ and a section $S$, placed between two hot plates is submitted to a temperature gradient $\Delta T$. A guard around the stack prevents heat losses through sample lateral surface. The heat flow across the sample $\phi$ is measured by a calorimeter under the stack.

*2.2.5. Specific heat capacity*

Modulated-Temperature Differential Scanning Calorimetry (MT-DSC) in quasi-isothermal conditions was used to determine composites specific heat capacity. Measurement were carried out at 19 °C, 34 °C and 48 °C on disks with a diameter of 6 mm, a thickness <500 μm and a mass ranging from 10 mg to 30 mg, encapsulated in an aluminium pan. An empty pan with matching mass was used as reference material.

A temperature modulation is superimposed to isotherms and the resulting modulated heat flow was recorded. MT-DSC enables to separate the in-phase and the out-of-phase responses from the total modulated heat flow. Far from thermal events, the specific heat capacity $C_p$ is proportional to the in-phase modulated heat flow amplitude $A_{HF}$ and the modulated temperature amplitude $A_T$ as in Eq. (6) [25].

$$C_p = K\frac{A_{HF}}{A_T} \tag{6}$$

$K$ is a calibration constant determined by a run with a sapphire standard. It accounts for thermal response of the reference, pans and furnace. Calibration runs were carried out before each run. Modulation parameters were 1 °C amplitude and 100 s period to ensure uniform heat flow across the sample [26].

*2.2.6. Thermal diffusivity*

The laser flash analyser LFA 447 from Netzsch was used to determine composites thermal diffusivity. Measurements were performed at 25 °C, 50 °C, 80 °C and 120 °C on square samples with a side dimension of 10 mm and a thickness superior to 2 mm coated with graphite on both sides. Thermal diffusivity α was calculated from the half temperature rise time $t_{1/2}$ according to Cape-Lehman model as in Eqs. (7) and (8) [27].

$$\alpha = \frac{e^2}{\pi^2 t_c} \tag{7}$$

$$\frac{t_{1/2}}{t_c} = g(1/2) \tag{8}$$

With e, the sample thickness, $t_c$ is the characteristic time necessary for the heat pulse to propagate through sample thickness, and $g(1/2)$ the value of $t/t_c$ at half temperature rise $\left(\frac{T(t)}{T_{\max}} = 0.5\right)$.

*2.2.7. Two-phases models for thermal conductivity*

*2.2.7.1. Maxwell model.* The Maxwell model is designed for composites where conductive particles are homogeneously dispersed in a continuous insulating matrix, in the case of spherical silver particles dispersed into PEEK matrix, the composite thermal conductivity according to Maxwell model is:

$$\lambda_{comp} = \lambda_{PEEK}\frac{\lambda_{Ag} + 2\lambda_{PEEK} + 2x\left(\lambda_{Ag} - \lambda_{PEEK}\right)}{\lambda_{Ag} + 2\lambda_{PEEK} + x\left(\lambda_{PEEK} - \lambda_{Ag}\right)} \tag{9}$$

In the case of oblong objects with an aspect ratio $\xi > 1$, Maxwell model is expressed as:

$$\lambda_{comp} = \lambda_{PEEK}\frac{3 + x(2\beta_{11}(1 - L_{11}) + \beta_{22}(1 - L_{33}))}{3 - x(2\beta_{11}L_{11} + \beta_{33}L_{33})} \tag{10-a}$$

With

$$\beta_{ii} = \frac{\lambda_{Ag} - \lambda_{PEEK}}{\lambda_{PEEK} + L_{ii}\left(\lambda_{Ag} - \lambda_{PEEK}\right)} \tag{10-b}$$

And

$$L_{11} = L_{22} = \frac{\xi^2}{2(\xi^2 - 1)} - \frac{\xi}{\left(2(\xi^2 - 1)\right)^{3/2}}\cosh^{-1}(\xi) \tag{10-c}$$

$$L_{33} = 1 - 2L_{11} \tag{10-d}$$

*2.2.7.2. Nan model.* Nan model derives from Maxwell model and includes interfacial thermal resistances [17], in this case the $\beta_{ii}$ term of Eq. (10) is replaced by:

$$\beta_{ii,NAN} = \frac{K_{ii} - \lambda_{PEEK}}{\lambda_{PEEK} + L_{ii}(K_{ii} - \lambda_m)} \tag{11-a}$$

In which

$$K_{ii} = \frac{\lambda_{Ag}}{1 + \gamma\frac{L_{ii}\lambda_{Ag}}{\lambda_{PEEK}}} \tag{11-b}$$

And for $\xi > 1$

$$\gamma = \left(2 + \frac{1}{\xi}\right)\frac{R_i\lambda_{PEEK}}{r} \tag{11-c}$$

$R_i$ is the adjustable parameter representing interface thermal resistance and $r$ is the nanowire radius. This model has been compared to experimental data in order to estimate interfacial thermal resistance between polymer and silver particles.

## 3. Results and discussions

### *3.1. Particles dispersion morphology*

Fig. 1 presents SEM images of PEEK/AgNP and PEEK/AgNWs composites. It shows the evolution of particles dispersion morphology from a homogeneous dispersion of silver particles (insets a and c) to a lightly aggregated system (insets b and d) when particles content increases. The presence of few particles aggregates and nanowires bundles is observed. These nanocomposites are still considered homogeneous. The dispersion morphology evolves more significantly for PEEK/AgNP composites filled above 13.5% as shown in Fig. 2. Silver particles are strongly aggregated and some paths of particles in close contact are visible.

### *3.2. Electrical conductivity*

Fig. 3 displays the evolution of DC electrical conductivity with increasing silver nanoparticles volume content of PEEK/AgNWs compared to PEEK/AgNP composites. In both cases, $\sigma_{DC}$ evolution is characteristic of electrical percolation. As conductive particle content increases, electrical conductivity increases sharply at a critical volume content associated with the percolation threshold. Above this threshold, composites electrical conductivity follows a power law:

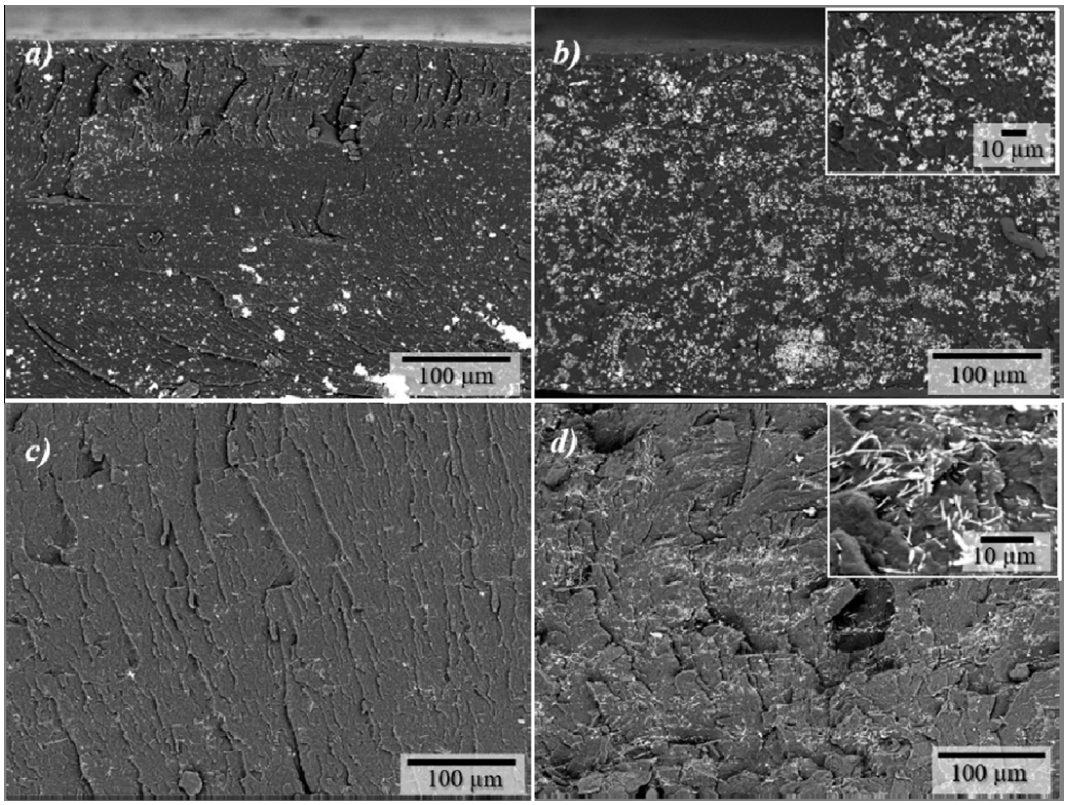


**Fig. 1.** SEM images of PEEK/Ag: a) PEEK+1.3 %vol AgNP, b) PEEK+7.7 %vol AgNP, c) PEEK+0.5 %vol AgNWs, d) PEEK+1.9 %vol AgNWs.

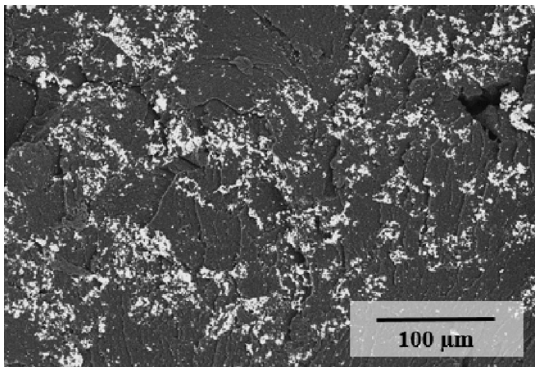


**Fig. 2.** SEM image of PEEK+13.5%AgNP.

$$\sigma = \sigma_0 (p - p_c)^t \tag{12}$$

In Eq. (12), $\sigma_o$ represents the particles network electrical conductivity, $p$ the particle volume content, $p_c$ their volume content at the percolation threshold and $t$ accounts for network dimensionality. The above mentioned fitting parameters strongly depend on dispersed phase nature and morphology. They are reported in Table 1.

Measurements of PEEK/AgNP composites electrical conductivity and discussions about the associated percolation law parameters are the subject of a previous work [28].

Concerning PEEK/AgNws nanocomposites, $\sigma_0$ is in good agreement with the measured electrical conductivity of compressed silver particles $\sigma_{AgNWs} \sim 10^5$ S m$^{-1}$. $\sigma_0$, accurately represents the electrical conductivity of AgNws nanoparticles network. The fitting parameter $t$ is also coherent with the theoretical range 1.60–2.00 for particles dispersed in the three dimensions.

From Fig. 3 and Table 1, appears a large difference between percolation thresholds of PEEK/AgNP ($p_c$ = 10.8 vol%) and PEEK/AgNWs ($p_c$ = 0.55 vol%) composites indicating that conductive pathways can be developed for significantly lower

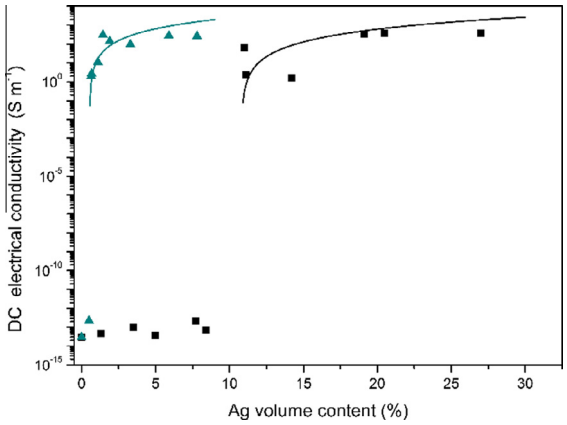


**Fig. 3.** DC electrical conductivity of PEEK/Ag nanocomposites as a function of Ag volume content at room temperature. (■) PEEK/AgNP nanocomposites [28], (▲) PEEK AgNWs nanocomposites. (–) Percolation law fit.

**Table 1**
Percolation law parameters for PEEK/AgNP [28] and PEEK/AgNWs composites.

| Percolation law parameters | PEEK/AgNP $\xi = 1$ | PEEK/AgNWs $\xi \sim 220$ |
|---|---|---|
| $\sigma_0$ (S m$^{-1}$) | $6.7 \cdot 10^4$ | $1.45 \cdot 10^5$ |
| $p_c$ (vol%) | 10.8 | 0.55 |
| $t$ (–) | 1.98 | 1.74 |

content with particles of higher aspect ratio. According to Balberg et al. [29], for capped cylinders, the percolation threshold can be linked to particles aspect ratio and anisotropy through their excluded volume $V_{ex}$. With the criterion of high aspect ratio randomly oriented nanowires, the total excluded volume $V_{ex}^{random}$ can be expressed as:

$$V_{ex}^{random} \cong 2\ \xi p_c = 1.41 \tag{13}$$

From Eq. (13), taking $p_c = 0.55$ vol% we calculated an apparent aspect ratio of 128. This aspect ratio is lower than the aspect ratio estimated from SEM image analysis, still of the same magnitude. This can be attributed to the deviation of the real nanowires dispersion from the randomly oriented case. Decreasing the degree of randomness may lead to an increase of the average total excluded volume and the percolation threshold [30].

### 3.3. Specific heat capacity

Fig. 4 displays the evolution of composites specific heat capacity with increasing silver content. No influence of particles aspect ratio is observed. In both cases, specific heat capacity decreases linearly with increasing particles weight content following the mixture rule:

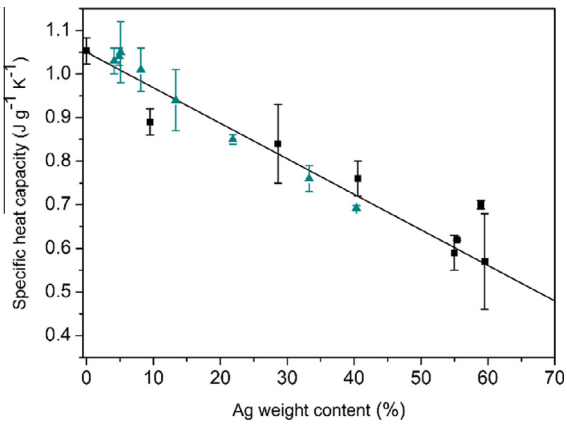


**Fig. 4.** Specific heat capacity of PEEK/Ag nanocomposites as a function of Ag volume content at 19 °C. (■) PEEK/AgNP nanocomposites, (▲) PEEK AgNWs nanocomposites, (–) Mixture rule.

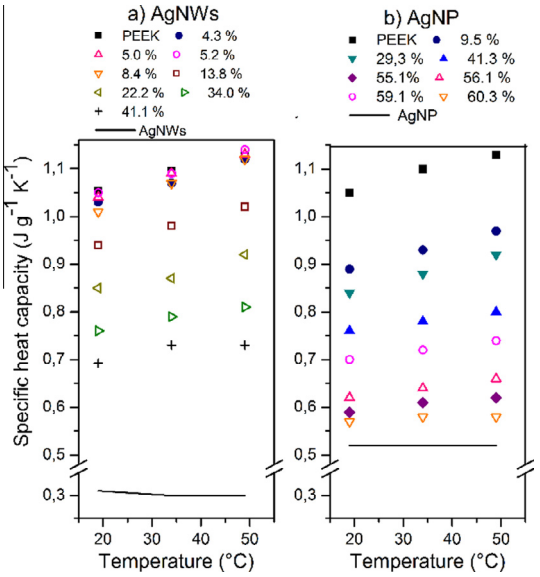


**Fig. 5.** Evolution of specific heat capacity with temperature: (a) PEEK/AgNWS composites, (b) PEEK/AgNP composites.

$$C_{p,composite} = wC_{p,Ag} + (1 - w)C_{p,PEEK} \tag{14}$$

With $w$ silver mass fraction, $C_{p,\mathrm{Ag}} = 0.235\ \mathrm{J\ g^{-1}\ K^{-1}}$ and $C_{p,\mathrm{PEEK}} = 1.053\ \mathrm{J\ g^{-1}\ K^{-1}}$.

The temperature dependence of composites specific heat capacity is exhibited in Fig. 5. Classically, specific heat capacity increases with temperature and reaches a plateau. At high temperature $C_p$ approaches the Dulong and Petit value. In semi-crystalline polymer, specific heat capacity temperature dependence is more pronounced than in metals [31]. As shown in Fig. 5 specific heat capacity of silver nanoparticles may be considered to be constant over the investigated temperature range while PEEK specific heat capacity visibly increases. Between these bounds, as silver content increases, temperature dependence of composites specific heat capacity decreases.

Data from Fig. 5 have been adjusted with a linear approximation. The slope of these linear approximations are reported in Fig. 6 as a function of particles content. Qualitatively, there is a downward trend of $C_p(T)$. Temperature dependence of heat capacity is less pronounced at high filler content. At a given silver content, the temperature dependence of composites specific heat capacity is independent of particle aspect ratio. $C_p(T)$ slope decreases with the same magnitude for PEEK/AgNP and PEEK/AgNWs. Composites ability to store thermal energy and its temperature dependence, only depends on components masses and respective specific heat capacities [32].

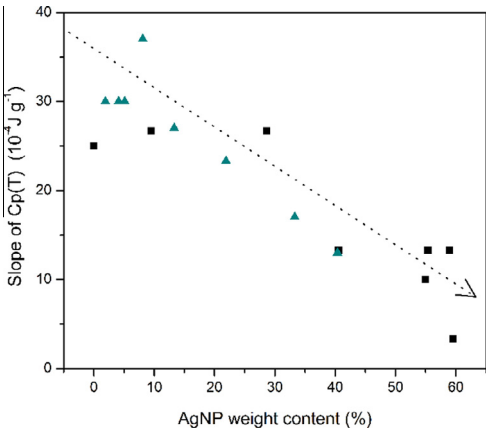


**Fig. 6.** Slope of Cp(T) linear approximation as a function of silver nanoparticles content: (■) PEEK/AgNP nanocomposites, (▲) PEEK/AgNWs nanocomposites. The dashed arrow is a guide line indicating the slope decrease.

### 3.4. Thermal conductivity

The comparative evolution of PEEK/AgNP and PEEK/AgNWs composites thermal conductivity with silver content is represented in Fig. 7. Thermal conductivity increases with increasing particle content. For a given particle content, thermal conductivity is higher with nanowires than with spherical nanoparticles: for 8 vol% silver, thermal conductivity of PEEK/AgNWs ($\lambda_{AgNWs\ (8\ vol\%)}$ = 1.08 W m$^{-1}$ K$^{-1}$) is twice higher than PEEK/AgNP composite ($\lambda_{AgNP\ (8\ vol\%)}$ = 0.49 W m$^{-1}$ K$^{-1}$).

For PEEK/AgNP composites below 5 vol%, our experimental data are in agreement with Maxwell model only for low filled composites. The discrepancy between experimental data and Maxwell model can be attributed to particles aggregates of higher aspect ratio. This statement is supported by the lower electrical percolation threshold observed compared to the 1416 vol% theoretical electrical percolation threshold for non-overlapping spherical particles [18]. The formation of higher aspect ratio aggregates called grapes [33] can develop paths of lower electrical and thermal resistances.

For PEEK/AgNWs composites, Maxwell model expressed for an aspect ratio of 128 overestimates experimental thermal conductivity. This model does not account for interface thermal resistances between particles and matrix. Taking $\xi$ = 128 and $R_i$ = 3.6 · 10$^{-6}$ m$^2$ K W$^{-1}$ Nan model is in good agreement with experimental data. This indicates that low thermal resistances pathways can been easily achieved with high aspect ratio nanowires but heat flux is hindered by rather large interface thermal resistances.

Evolution of thermal conductivity with temperature is an indication of the dominant heat transport mechanism. It is interesting to know whether thermal conductivity increases or decreases with temperature. The first scenario indicates a

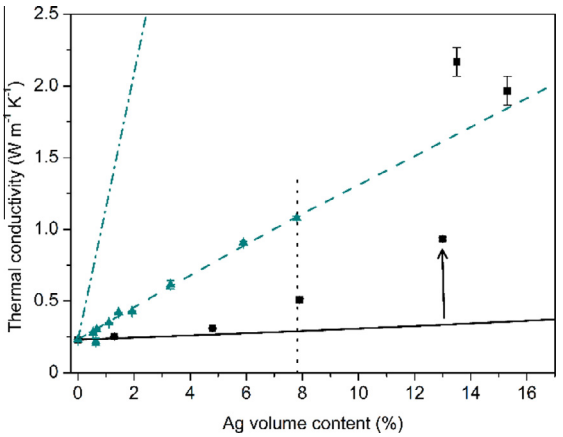


**Fig. 7.** Thermal conductivity of PEEK/Ag nanocomposites as a function of Ag volume content at 25 °C. (■) PEEK/AgNP nanocomposites, (▲) PEEK AgNWs nanocomposites, (—) Maxwell model ($\xi$ = 1), (— ■ —) Maxwell model ($\xi$ = 128) and (- - - -) Nan model with $\xi$ = 128 and $R_i$ = 3.6 · 10$^{-6}$ m$^2$ K W$^{-1}$.

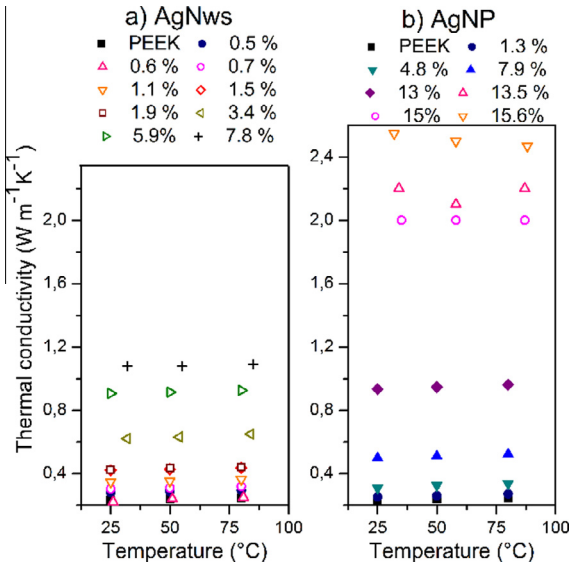


**Fig. 8.** Evolution of thermal conductivity with temperature: (a) PEEK/AgNWS composites, (b) PEEK/AgNP composites.

limited phonon mean free path and a dominant contribution of increasing heat capacity; mechanism attributed to disordered materials [31,34]. The second scenario indicates heat flow is damped through phonon scattering as temperature increases, and a nearly constant heat capacity; mechanism attributed to crystalline materials [35,36]. In Fig. 8, we plotted thermal conductivities of PEEK/Ag nanocomposites as a function of temperature. Composites thermal conductivity slightly increases with temperature for PEEK/AgNWs and PEEK/AgNP. There is a different behaviour for composites filled with 13.5 % AgNP, and 15.6 %AgNP. For the first one, thermal conductivity decreases then increases, for the second one thermal conductivity decreases when temperature increases.

The introduction of metallic filler does not modify the temperature dependence of composites thermal conductivity. PEEK/Ag composites as a whole, behave like disordered material. The exception of composite filled above 13.5 vol% AgNP for which thermal conductivity decreases as temperature increases, can be explained by metallic aggregates in close contact as in Fig. 2. In these aggregates, phonons are more scattered as temperature increases. This hypothesis is supported by the high thermal conductivity of these composites and the thermal conductivity discontinuity in this region as shown in Fig. 7. Aspect ratio has no influence on heat transport mechanisms at a macroscopic scale. PEEK/AgNP and PEEK/AgNWs have the same behaviour. This result can be linked to the fact that specific heat capacity does not depend on aspect ratio and composites thermal conductivity evolution with respect to temperature is dominated by specific heat evolution.

### *3.5. Thermal diffusivity*

Fig. 9 represents composites thermal diffusivity as a function of silver nanoparticles volume content; it exhibits the comparison between measured thermal diffusivity (filled symbols) and calculated thermal diffusivity (open symbols) according to Eq. (4).

First of all, measured and calculated thermal diffusivities are in good agreement excepted for composites filled with 13.5 vol% and 15.5 vol% AgNP. The discrepancy at high filler content can be attributed to heterogeneities. Laser flash analysis, modulated temperature differential calorimetry and the guarded hot plates method, represent different thermal measurement scales. The first method is transitory, the second is quasi-stationary and the last is stationary. There is a coherence of thermal responses at different measurement scales for homogeneous composites.

Composites thermal diffusivity increases with increasing particle content and the influence of particle aspect ratio is also observable. Higher thermal diffusivity is reached with silver nanowires for a given particle content.

Fig. 10 displays the evolution of thermal diffusivity with temperature and shows that thermal diffusivity decreases with temperature for every composites. It can be seen that temperature dependance of thermal diffusivity is more ronouced as silver content increases. Experimental thermal diffusivity decreases as $T^{-b}$ with $b$ varying between 0.3 and 0.8. Exponent $b$ increases when silver nanoparticles content increases. Choy et al. [37] reported a similar behaviour in semi-crystalline polymers; thermal diffusivity decreased as $T^{-b}$ with $b$ ranging 0.5–1 and a stronger temperature dependance was observed for polymers of higher initial thermal diffusivity. Thermal diffusivity is related to temperature variations kinetic; at microscopic scale it only depends on phonon mean free path and sound velocity (Debye expression). As temperature increases, thermal diffusivity decreases because phonon mean free path decreases. Consequently, the positive temperature dependance of composites thermal conductivity indicates that heat transport is dominated by increasing specific heat capacity with temperature rather than decreasing phonon mean free path. This behaviour is typical of disordered materials.

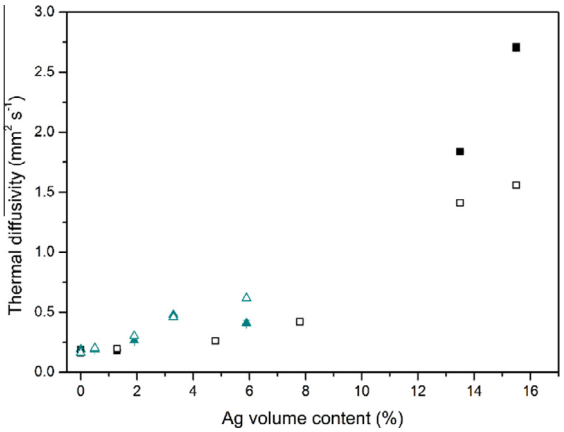


**Fig. 9.** Thermal diffusivity of PEEK/Ag nanocomposites as a function of Ag volume content at 25 °C. (■) PEEK/AgNP nanocomposites, (▲) PEEK AgNWs nanocomposites. Measured by LFA (filled symbols) vs calculated according to Eq. (4) (open symbols).

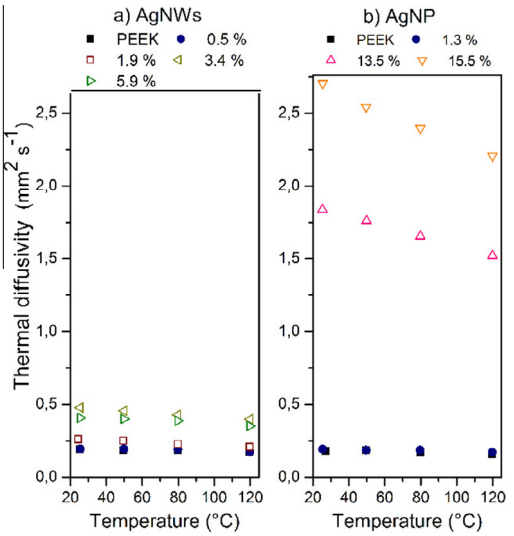


**Fig. 10.** Evolution of thermal diffusivity with temperature: (a) PEEK/AgNWS composites, (b) PEEK/AgNP composites.

## 4. Conclusions

In this study, influence of silver nanoparticle aspect ratio on electrical and thermal transport has been investigated in PEEK/Ag composites. A low percolation threshold has been obtained with silver nanowires (0.55 vol%) compared to silver nanospheres (10.8 vol%). Percolation law fitting parameters indicate a randomly oriented nanowires dispersion in the three dimensions. Specific heat capacity is independent of particles aspect ratio; it decreases following the mixture rule as silver weight content increases. Temperature dependence of composites specific heat capacity is of the same magnitude for PEEK/AgNP and for PEEK/AgNWs. The ability of composites to store energy only depends on particle weight content and components respective specific heat capacities. Higher thermal conductivity and thermal diffusivity are reached with silver nanowires for a given particle content. This trend asserts the interest of high aspect ratio silver particles to optimize both electrical and thermal properties in thermostable thermoplastic based composites.

At macroscopic scale, thermal transport is attributed to the same mechanisms for PEEK/AgNP and PEEK/AgNWs composites. As particle content increases, temperature dependence of specific heat capacity weakens. On the contrary, thermal diffusivity decreases more sharply with temperature when silver content increases. Moreover, positive temperature dependence of thermal conductivity is unmodified by increasing amount of silver particles and is due to the dominant contribution of increasing heat capacity with temperature.

## Acknowledgements

This work was done in the framework of the MACOTHEC program and supported by Bpifrance and Conseil Regional Midi Pyrénées.

## References

[1] S. Kirkpatrick, Percolation and conduction, Rev. Mod. Phys. 45 (1973) 574–588, http://dx.doi.org/10.1103/RevModPhys.45.574.
[2] P. Sheng, Fluctuation-induced tunneling conduction in disordered materials, Phys. Rev. B 21 (1980) 2180–2195, http://dx.doi.org/10.1103/PhysRevB.21.2180.
[3] W. Thongrunag, C.M. Balik, R.J. Spontak, Volume-exclusion effects in polyethylene blends filled with carbon black, graphite, or carbon fiber, J. Polym. Sci., Part B: Polym. Phys. 40 (2002) 1013–1025, http://dx.doi.org/10.1002/polb.10157.
[4] W. Bauhofer, J.Z. Kovacs, A review and analysis of electrical percolation in carbon nanotube polymer composites, Compos. Sci. Technol. 69 (2009) 1486–1498, http://dx.doi.org/10.1016/j.compscitech.2008.06.018.
[5] A. Lonjon, I. Caffrey, D. Carponcin, E. Dantras, C. Lacabanne, High electrically conductive composites of Polyamide 11 filled with silver nanowires: nanocomposites processing, mechanical and electrical analysis, J. Non Cryst. Solids 375 (2013) 199–204, http://dx.doi.org/10.1016/j.jnoncrysol.2013.05.020.
[6] A. Lonjon, P. Demont, E. Dantras, C. Lacabanne, Low filled conductive P(VDF-TrFE) composites: influence of silver particles aspect ratio on percolation threshold from spheres to nanowires, J. Non Cryst. Solids 358 (2012) 3074–3078, http://dx.doi.org/10.1016/j.jnoncrysol.2012.09.006.
[7] L. Quiroga Cortes, A. Lonjon, E. Dantras, C. Lacabanne, High-performance thermoplastic composites poly(ether ketone ketone)/silver nanowires: morphological, mechanical and electrical properties, J. Non Cryst. Solids 391 (2014) 106–111, http://dx.doi.org/10.1016/j.jnoncrysol.2014.03.016.
[8] B. Weidenfeller, M. Höfer, F.R. Schilling, Thermal conductivity, thermal diffusivity, and specific heat capacity of particle filled polypropylene, Compos. Part A Appl. Sci. Manuf. 35 (2004) 423–429, http://dx.doi.org/10.1016/j.compositesa.2003.11.005.
[9] Y. Mamunya, V.V. Davydenko, P. Pissis, E. Lebedev, Electrical and thermal conductivity of polymers filled with metal powders, Eur. Polym. J. 38 (2002) 1887–1897, http://dx.doi.org/10.1016/S0014-3057(02)00064-2.

[10] S. Kume, I. Yamada, K. Watari, I. Harada, K. Mitsuishi, High-thermal-conductivity AlN filler for polymer/ceramics composites, J. Am. Ceram. Soc. 92 (2009) S153–S156, http://dx.doi.org/10.1111/j.1551-2916.2008.02650.x.
[11] A. Boudenne, L. Ibos, M. Fois, E. Gehin, J.C. Majeste, Thermophysical properties of polypropylene/aluminum composites, J. Polym. Sci. Part B – Polym. Phys. 42 (2004) 722–732, http://dx.doi.org/10.1002/polb.10713.
[12] N. Abdel-Aal, F. El-Tantawy, A. Al-Hajry, M. Bououdina, Epoxy resin/plasticized carbon black composites. Part I. Electrical and thermal properties and their applications, Polym. Compos. 29 (2008) 511–517, http://dx.doi.org/10.1002/pc.20401.
[13] C.L. Choy, K.W. Kwok, W.P. Leung, F.P. Lau, Thermal conductivity of poly(ether ether ketone) and its short-fiber composites, J. Polym. Sci., Part B: Polym. Phys. 32 (1994) 1389–1397, http://dx.doi.org/10.1002/polb.1994.090320810.
[14] Z. Han, A. Fina, Thermal conductivity of carbon nanotubes and their polymer nanocomposites: a review, Prog. Polym. Sci. 36 (2011) 914–944, http://dx.doi.org/10.1016/j.progpolymsci.2010.11.004.
[15] F.H. Gojny, M.H.G. Wichmann, B. Fiedler, I.A. Kinloch, W. Bauhofer, A.H. Windle, et al, Evaluation and identification of electrical and thermal conduction mechanisms in carbon nanotube/epoxy composites, Polymer 47 (2006) 2036–2045, http://dx.doi.org/10.1016/j.polymer.2006.01.029.
[16] M.J. Biercuk, M.C. Llaguno, M. Radosavljevic, J.K. Hyun, a.T. Johnson, J.E. Fischer, Carbon nanotube composites for thermal management, Appl. Phys. Lett. 80 (2002) 2767–2769, http://dx.doi.org/10.1063/1.1469696.
[17] C.-W. Nan, R. Birringer, D.R. Clarke, H. Gleiter, Effective thermal conductivity of particulate composites with interfacial thermal resistance, J. Appl. Phys. 81 (1997) 6692, http://dx.doi.org/10.1063/1.365209.
[18] C.-W. Nan, Physics of inhomogeneous inorganic materials, Prog. Mater. Sci. 37 (1993) 1–116, http://dx.doi.org/10.1016/0079-6425(93)90004-5.
[19] J.-L. Zeng, F.-R. Zhu, S.-B. Yu, L. Zhu, Z. Cao, L.-X. Sun, et al, Effects of copper nanowires on the properties of an organic phase change material, Sol. Energy Mater. Sol. Cells 105 (2012) 174–178.
[20] J. Zeng, Z. Cao, D.W. Yang, L.X. Sun, L. Zhang, Thermal conductivity enhancement of Ag nanowires on an organic phase change material, J. Therm. Anal. Calorim. 101 (2010) 385–389, http://dx.doi.org/10.1007/s10973-009-0472-y.
[21] W.H. Chen, H.C. Cheng, Y.C. Hsu, R.H. Uang, J.S. Hsu, Mechanical material characterization of Co nanowires and their nanocomposite, Compos. Sci. Technol. 68 (2008) 3388–3395, http://dx.doi.org/10.1016/j.compscitech.2008.09.030.
[22] K. Razeeb, E. Dalton, Advances in Nanocomposites – Synthesis Characterization and Industrial Applications, In Tech, Rijeka, 2011. <www.intechopen.com/books/advances-in-nanocomposites-synthesis-characterization-and-industrial-applications/naowire-polymer-nanocoposites-as-thermail-interface-material>.
[23] S.W. Hughes, Archimedes revisited: a faster, better, cheaper method of accurately measuring the volume of small objects, Phys. Educ. 40 (2005) 468–474, http://dx.doi.org/10.1088/0031-9120/40/5/008.
[24] H.E. Bair, W.E. Bessey, R.P. Chartoff, P.K. Gallagher, A. Hale, M. Jaffe, et al, Thermal Characterization of Polymeric Materials, second ed., Academic Press, San Diego, 1997.
[25] A. Boller, Y. Jin, B. Wunderlich, Heat capacity measurement by modulated DSC at constant temperature, J. Therm. Anal. 42 (1994) 307–330, http://dx.doi.org/10.1007/BF02548519.
[26] L.C. Thomas, Measurement of Accurate Heat Capacity Values, TA Instruments, Modul. DSC Pap. #9. (2005) 1–11.
[27] J.A. Cape, G.W. Lehman, Temperature and finite pulse-time effects in the flash method for measuring thermal diffusivity, J. Appl. Phys. 34 (1963) 1909–1913, http://dx.doi.org/10.1063/1.1729711.
[28] L. Riviere, N. Causse, A. Lonjon, É. Dantras, C. Lacabanne, L. Rivière, et al, Specific heat capacity and thermal conductivity of PEEK/Ag nanoparticles composites determined by Modulated-Temperature Differential Scanning Calorimetry, Polym. Degrad. Stab. 127 (2016) 98–104, http://dx.doi.org/10.1016/j.polymdegradstab.2015.11.015.
[29] I. Balberg, N. Binenbaum, N. Wagner, Percolation thresholds in the three-dimensional sticks system, Phys. Rev. Lett. 52 (1984) 1465–1468, http://dx.doi.org/10.1103/PhysRevLett.52.1465.
[30] I. Balberg, C.H. Anderson, S. Alexander, N. Wagner, Excluded volume and its relation to the onset of percolation, Phys. Rev. B 30 (1984) 3933–3943, http://dx.doi.org/10.1103/PhysRevB.30.3933.
[31] D.G. Cahill, R.O. Pohl, Lattice vibrations and heat transport in crystals and glasses, Annu. Rev. Phys. Chem. 39 (1988) 93–121, http://dx.doi.org/10.1146/annurev.physchem.39.1.93.
[32] B. Budiansky, Thermal and thermoelastic properties of isotropic composites, J. Compos. Mater. 4 (1970) 286–295, http://dx.doi.org/10.1177/002199837000400301.
[33] A.I. Medalia, Electrical conduction in carbon black composites, Rubber Chem. Technol. 59 (1986) 432–454, http://dx.doi.org/10.5254/1.3538209.
[34] C. Kittel, Interpretation of the thermal conductivity of glasses, Phys. Rev. 75 (1949) 972–974, http://dx.doi.org/10.1103/PhysRev.75.972.
[35] C. Kittel, Introduction to Solid State Physics, third ed., Wiley, John, New York, 1967.
[36] C. Uher, Thermal Conductivity, Theory, Properties and Applications: Thermal Conductivity of Metals, 2004.
[37] C.L. Choy, E.L. Ong, F.C. Chen, Thermal diffusivity and conductivity of crystalline polymers, J. Appl. Polym. Sci. 26 (1981) 2325–2335, http://dx.doi.org/10.1002/app.1981.070260719.